Application of a classical PD regulator to the control of a flexible planar closed chain linkage

Alessandro Gasparetto* Stefano Miani†

DIEGM, Università degli Studi di Udine,
Via delle Scienze 208, 33100 Udine, Italy

Abstract

This paper presents an approach to the control of a flexible planar closed-chain linkage. A very accurate dynamic model of the system is briefly summarized. Such a model is then employed to test a classical PD regulator in simulation to control a flexible planar four-bar linkage. The chosen PD control is described, and the most significant results of the simulation are presented and discussed.

1 Introduction

In the recent years, the interest for flexible linkages has greatly risen in the field of robotics, because operations at increasingly high speed are requested to manipulators. In order to meet such strict dynamic requirements, new, lighter robot manipulators ought to be designed and realized. The main problem preventing a widespread diffusion of light robots lies in the fact that the links of such robots do not show a rigid-body behavior; hence, vibratory phenomena need to be taken into account and accurately modeled and controlled. Such a problem seriously affects the manipulator performances, because oscillations persist for a certain period of time even after the desired position has been reached. Many techniques have been proposed in the last years to reduce vibrations of flexible linkages. Bayo *et al.* (1989) use an iterative frequency domain approach based on inverse dynamics. Lee and Jee (1996) propose an H_∞ robust control of a flexible slewing beam. Milford and Asokanthan (1994) use an adaptive control. Takashi and Yamada (1994) use a neural network to control a single-link flexible arm. Yigit (1994) investigates the stability of a PD control for a two-link rigid-flexible manipulator. However, most of the works in this field apply to single-link or a two-link planar manipulators. Multiple-link closed chain manipulators have been less investigated so far, mainly because building an accurate dynamic model proved to be a very challenging task. Dynamic models for flexible multiple-link manipulators have been proposed by Turcic and Midha (1984), Yang and Park (1996) and Giovagnoni (1994). Controls of flexible multiple-link manipulators have been proposed for instance by Lopez-Linares *et al.* (1997). In this paper, the application of a classical PD regulator to the control of a flexible planar closed-chain four-bar linkage is presented. The dynamical model used is the one proposed by Giovagnoni (1994), and it will be summarized in Section 2. In Section 3 the designed PD control is described, and in Section 4 the most significant results of simulations are reported and discussed. In Section 5 some concluding remarks are given.

*Email: *gasparetto@uniud.it*
†Email: *miani.stefano@uniud.it*

2 Dynamic model

The dynamic model considered is taken from Giovagnoni (1994), who proposed an accurate dynamic model of a flexible multi-body system. In this Section we will just summarize the model and provide the resulting equations, which are valid for whatever multi-body flexible planar linkage.

In the model, the total link motion is separated into a rigid motion and the elastic displacement of any point of the system with respect to a rigid-link system, named ERLS (Equivalent Rigid Link System). Referring to Figure 1, the total nodal motion b_i of the i-th element is given by the sum of the rigid motion r_i of the node, belonging to the ERLS, and the nodal elastic displacement u_i:

$$b_i = r_i + u_i \tag{1}$$

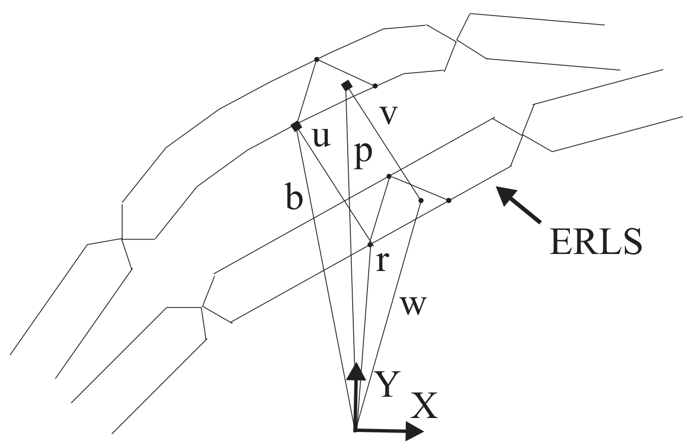

Figure 1: Flexible link model

The displacements of all nodes can then be assembled into a unique vector, so that it is possible to rewrite the equation above in vector form as

$$\mathbf{b} = \mathbf{r} + \mathbf{u} \tag{2}$$

The kinematics of the ERLS is determined according to the ordinary rules for a chain of rigid links. Hence, the vector $\mathbf{q}$, containing the generalized coordinates (i.e. the degrees of freedom) of the ERLS, completely defines the position of the rigid system. The rigid nodal velocities and accelerations can then be expressed as functions of the velocities and accelerations of the generalized coordinates of the ERLS, by virtue of the matrix of the sensitivity coefficients $S(\mathbf{q})$:

$$\dot{\mathbf{r}} = S(\mathbf{q})\dot{\mathbf{q}} \tag{3}$$

$$\ddot{\mathbf{r}} = S(\mathbf{q})\ddot{\mathbf{q}} + \dot{S}(\mathbf{q}, \dot{\mathbf{q}})\dot{\mathbf{q}} \tag{4}$$

where $\dot{\mathbf{r}}$, $\ddot{\mathbf{r}}$ are respectively the vectors of the rigid velocities and accelerations for all the nodes. $S(\mathbf{q})$, namely the sensitivity coefficient matrix for all the nodes, is an explicit function of $\mathbf{q}$, and its columns contain the rigid-body velocities corresponding to unit velocities of the generalized coordinates of the ERLS.

The model then considers each flexible link to be subdivided into finite elements. For any generic point inside the finite element considered, the position vector p_i is the sum of the position vector w_i of the point in the ERLS and of its elastic displacement vector v_i:

$$p_i = w_i + v_i \tag{5}$$

The displacements inside the finite elements are defined using adequate interpolation functions, according to the finite elements theory.

Then, once the system kinematics has been defined, the differential equations of motion for the flexible system are obtained by expressing the dynamic equilibrium of the system thru the virtual work principle (again, refer to (Giovagnoni, 1994) for an exhaustive proof). A set of coupled equations for the dynamic analysis of a chain of flexible bodies is thus obtained, namely the following system of differential equations (where we have removed the dependence from the generalized coordinates $\mathbf{q}$ for clarity):

$$M(\ddot{\mathbf{r}} + \ddot{\mathbf{u}}) + 2M_c\dot{\mathbf{u}} + \alpha M\dot{\mathbf{u}} + \beta K\dot{\mathbf{u}} + K\mathbf{u} = \mathbf{f}_g + \mathbf{f} \tag{6}$$

$$S^T M(\ddot{\mathbf{r}} + \ddot{\mathbf{u}}) + 2S^T M_c\dot{\mathbf{u}} + \alpha S^T M\dot{\mathbf{u}} = S^T(\mathbf{f}_g + \mathbf{f}) \tag{7}$$

where the elements appearing in the above equations are defined as follows:

- $\dot{\mathbf{u}}$, $\ddot{\mathbf{u}}$ are respectively the vectors of the elastic velocities and accelerations for all nodes;
- M is the mass matrix for all elements, which is built by assembling the mass matrices for each element, obtained by integrating the elements' densities over their volumes;
- M_c is the matrix arising from Coriolis contributions;
- K is the stiffness matrix for all elements, built by assembling the stiffness matrices of all elements;
- $\mathbf{f}_g$ is the vector of the generalized gravity forces;
- $\mathbf{f}$ is the vector of the generalized external loads;
- α and β are the Rayleigh damping coefficients.

The system of differential equations (6)-(7) expressing the dynamics of the linkage is divided into two subsystems. Equation (6) expresses the nodal equilibrium for all nodes, namely the equivalent loads applied on every node must be in equilibrium. Equation (7) expresses the overall equilibrium of the ERLS, i.e. all the equivalent nodal loads applied to the linkage must produce no work for a virtual displacement of the ERLS.

The system (6)-(7) can then be further rearranged, by expressing the vector $\mathbf{r}$ as a function of the generalized accelerations and velocities of the ERLS through the matrix of the sensitivity coefficients:

$$\ddot{\mathbf{r}} = S\ddot{\mathbf{q}} + (\sum_j \dot{q}_j \frac{\partial S}{\partial q_j})\dot{\mathbf{q}} \tag{8}$$

Thus, Eqs. (6)-(7) can be rewritten as:

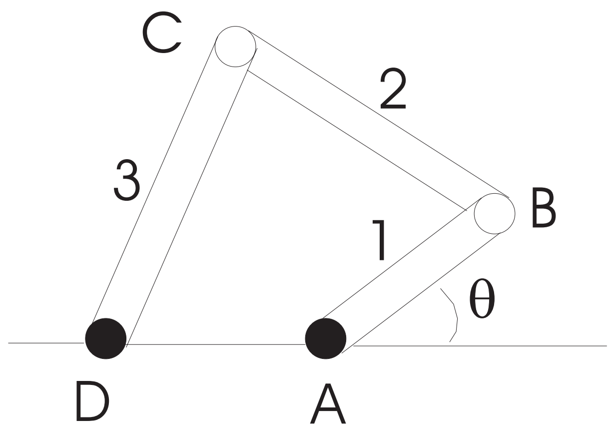

Figure 2: Flexible four bar linkage under test

$$M\ddot{\mathbf{u}} + MS\ddot{\mathbf{q}} = \mathbf{t}(\mathbf{u}, \dot{\mathbf{u}}, \mathbf{q}, \dot{\mathbf{q}}) \tag{9}$$

$$S^T M\ddot{\mathbf{u}} + S^T MS\ddot{\mathbf{q}} = S^T\mathbf{t}(\mathbf{u}, \dot{\mathbf{u}}, \mathbf{q}, \dot{\mathbf{q}}) \tag{10}$$

where $\mathbf{t}$ accounts for all the forces excluding those directly related to the second derivatives of the generalized coordinates.

From Eqs. (9)-(10) it is straightforward to obtain a system that enables one to directly compute the elastic accelerations $\ddot{\mathbf{u}}$ and the accelerations of the generalized coordinates $\ddot{\mathbf{q}}$:

$$\begin{bmatrix} M & MS \\ S^T M & S^T MS \end{bmatrix} \begin{bmatrix} \ddot{\mathbf{u}} \\ \ddot{\mathbf{q}} \end{bmatrix} = \begin{bmatrix} \mathbf{t} \\ S^T\mathbf{t} \end{bmatrix} \tag{11}$$

Once the accelerations $(\ddot{\mathbf{u}}, \ddot{\mathbf{q}})$ are computed, the velocities $(\dot{\mathbf{u}}, \dot{\mathbf{q}})$ and displacements $(\mathbf{u}, \mathbf{q})$ of the system can be obtained by integration, using for example the Runge-Kutta method. The model described in this Section proved to be very accurate in reproducing the dynamic behavior of a chain of flexible link. Namely, the results of simulation tests were in excellent agreement with experimental data (Giovagnoni, 1994).

3 The PD Control

The model built in the former Section provides a very powerful tool to evaluate the dynamic variables of the system (accelerations, velocities and displacements of the generalized coordinates and of the nodes). Hence, no estimator of any sort needs to be employed to evaluate the system dynamics, when applying a control in simulation. The test case used in our simulations is a four-link closed-chain planar manipulator (see Figure 2), set in a horizontal plane so as to neglect the gravity effects. Its mechanical features are:

Links lengths

- AB = 0.360 m
- BC = 0.528 m
- CD = 0.636 m

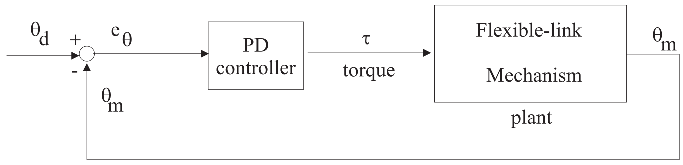

Figure 3: Control scheme

- DA = 0.332 m (fixed frame)

Masses and inertia

- concentrated inertia at joint A=$3.971 \times 10^{-4} kg\ m^2$
- concentrated mass at joint B=0.040 kg
- concentrated mass at joint C=0.040 kg
- concentrated inertia at joint D=$1.656 \times 10^{-4} kg\ m^2$
- linearly distributed mass of the links = 0.272 kg/m

The realized PD control has been implemented in the Matlab-Simulink simulation environment. The scheme of the control is shown in Figure 3.

The "plant" block is a function realized in the Matlab language, that simulates the mechanical behavior of the system according to the model described in Section 2. Due to the fact that the system dynamics are obtained thru finite elements method, we couldn't derive a nonlinear explicit expression relating the inputs with the nodal coordinates of the form

$$\dot{x} = f(x, u)$$

(the problem of interpolating a set of overdetermined nonlinear equations by means of a single "standard" nonlinear differential equation is currently under investigation). Thus, as a first step, we considered a simple PD controller with the primary objective of stabilizing the rigid motion of the structure while trying to reduce the numerous oscillatory modes present in the flexible structure. A preliminary analysis of the behavior of the linearized system for values of the free

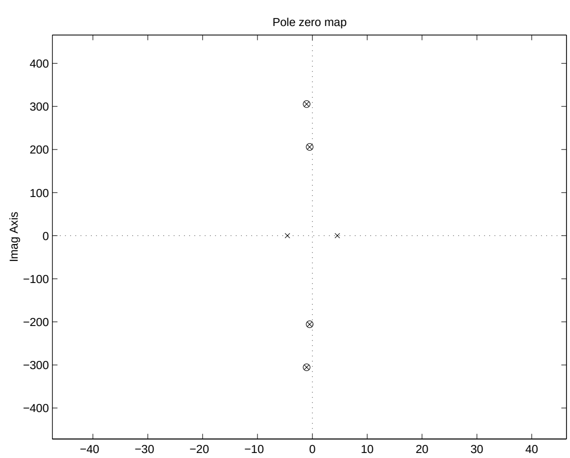

Figure 4: Complex plane location of poles and zeros for $\theta = 1$ rad

coordinate in the range $[0, 1]$ rad via simulation evidenced, in accordance with the theoretical model, the presence of a first oscillatory mode at about 33 Hz and of a secondary oscillatory mode whose frequency is at about 48 Hz. The transfer function from the torque input to the free coordinate of the flexible structure can thus roughly be approximated with two 0-symmetric real poles, two couples of complex poles accompanied by two couples of complex zeros. Based on this we designed a simple PD structure which was approximated with a zero-pole structure, with the zero at $-\frac{50}{6}$, the pole at -50 and a static gain of $K = 10$. The two experimentally derived couples of poles and zeros along with the two real poles for a steady state configuration of the mechanism corresponding to a value of the free coordinate equal to 1 rad, are shown in figure 4.

4 Simulation results

All the simulations were run on a 300 MHz pentium and we used the Matlab-Simulink environment with integration method Runge-Kutta, fixed step with a 10^{-6} tolerance. The first case we considered is that in which the system is fed a step reference value. We report in Figures 5,6 and 7 the dynamic behavior of the free coordinate, the vertical displacement of the midpoint of link 2, and the applied torque, respectively. Note that, due to the high gain used, the torque tends to assume exceedingly large values (thus a saturation block should have been introduced) and this in turn significantly excites the first oscillatory mode, as evidenced by figure 6, which affects, in accordance with experimental results in Giovagnoni (1994), the free coordinate motion.

We then considered a filtered step input, where the filter is obtained by cascading two first

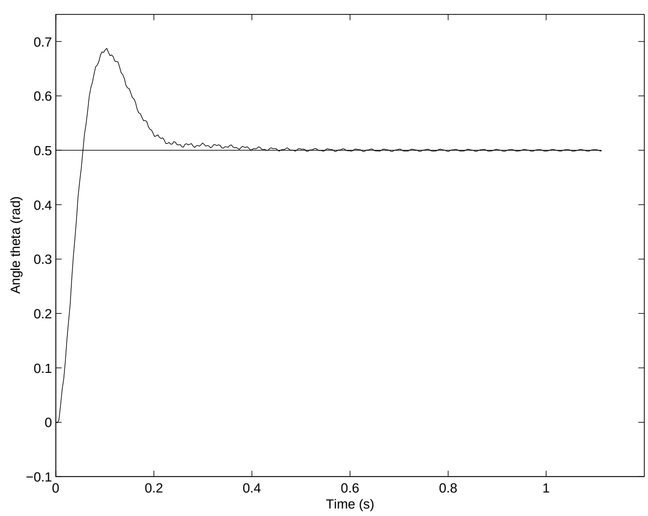

Figure 5: Free coordinate, step response

order filters with poles at $p = -10 \pm 2\sqrt{5}$. The advantages of this are evidenced in figures 8,9 and 10: the smoother transition from zero to the reference value prevents the oscillatory modes from being exceedingly excited, allows the system to better track the imposed input without overshoot, and reduces by a factor of 30 the value of the applied torque. The payoff is obviously given by a slower, although still reasonable, convergence to the steady state value.

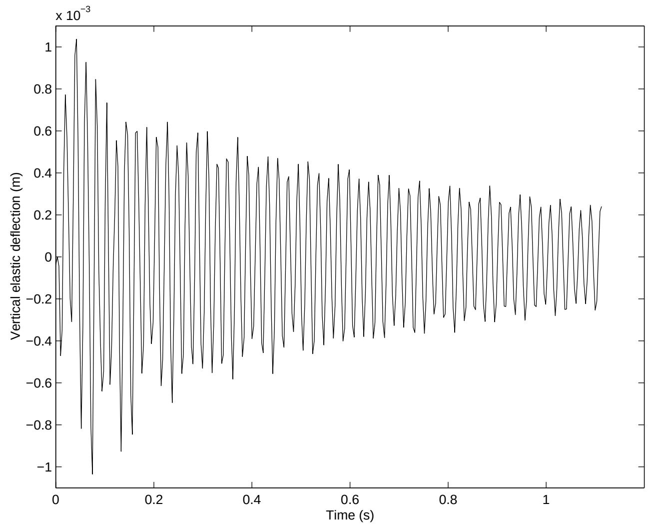

Figure 6: Midspan of link 2, vertical elastic displ., step response

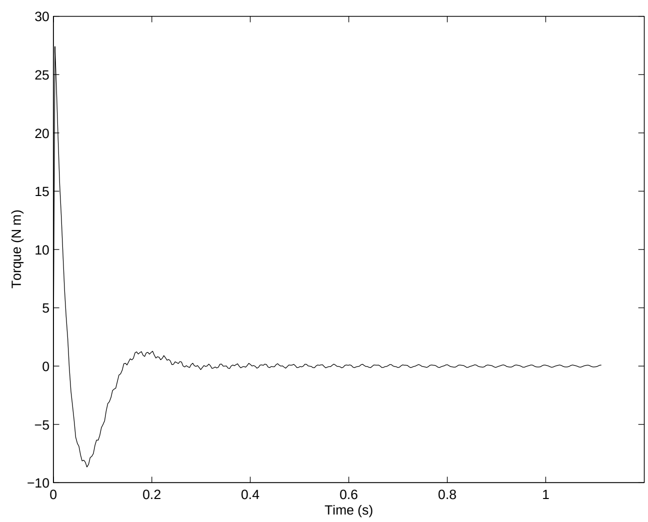

Figure 7: Applied torque, step response

5 Conclusions

In this paper we reported the simulated results of the application of a simple PD controller to a flexible planar closed chain four-bar linkage. Much emphasis was put on the excellent agreement of the simulated results with the experimental behaviour of the real system, which allows the designer to use the simulated model to effectively test whatever type of control structure. The realized Matlab-Simulink function is still rather time-consuming (each simulation took roughly 1 hour on a 300 MHz Pentium) and further work is in the direction of developing a faster approximated nonlinear model in explicit state space form allowing to perform synthesis of more complex control structures which will be tested experimentally on a real flexible four-bar linkage.

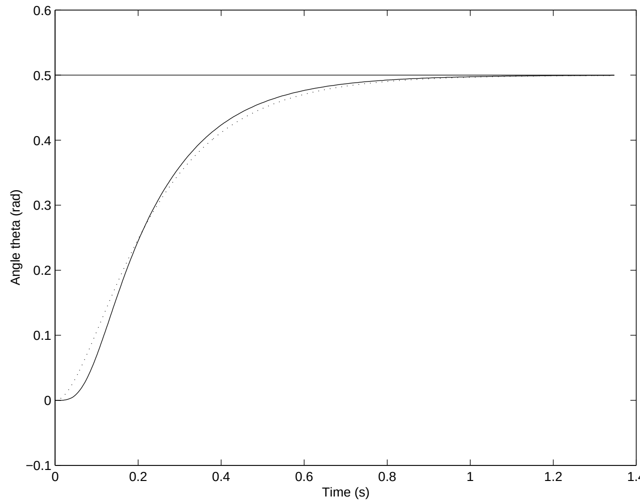

Figure 8: Free coordinate, filtered step response

References

Bayo, E., P. Papadopoulos, and J. Stubbe (1989). "Inverse Dynamics and Kinematics of Multi-Link Elastic Robots: An Iterative Frequency Domain Approach," *The International Journal of Robotic research*, **8**, no. 6, pp. 49–62.

Lee, C. W., and W. H. Jee (1996). "H_∞ Robust Control of Flexible Beam Vibration by Using a Hybrid Damper", *ASME Journal of Dynamic Systems, Measurement and Control*, **118**, pp. 643–648.

Milford, R. I., and S. F. Asokanthan (1994). "Experimental On-Line Frequency Domain Identification and Adaptive Control of a Flexible Slewing Beam", *ASME Journal of Dynamic Systems, Measurement and Control*, **118**, pp. 58–65.

Takahashi, K., and I. Yamada (1994) "Neural-Network Based Learning Control of Flexible Mechanism With Application to a Single-Link Flexible Arm", *ASME Journal of Dynamic Systems, Measurement and Control*, **116**, pp. 792–795.

Yigit, A. S. (1994). "On the Stability of PD Control for a Two-Link Rigid-Flexible Manipulator", *ASME Journal of Dynamic Systems, Measurement and Control*, **116**, pp. 208–215.

Turcic, D. A., and A. Midha (1984). "Generalized Equations of Motion for the Dynamic Analysis of Elastic Mechanism Systems", *ASME Journal of Dynamic Systems, Measurement and Control*, **106**, pp. 243–248.

Yang, K. H., and Y. S. Park (1996), "Dynamic Stability Analysis of a Closed-Loop Flexible-Link Mechanism", *Mechanism and Machine Theory*, **31**, no. 5, pp. 545–560.

Giovagnoni, M. (1994). "A Numerical and Experimental Analysis of a Chain of Flexible Bodies", *ASME Journal of Dynamic Systems, Measurement and Control* **116**, pp. 73–80.

Lopez-Linares, S., A. Konno, and M. Uchiyama (1997). "Vibration Suppression Control of 3D Flexible Robots Using Velocity Inputs", *Journal of Robotic Systems*, **14**, no. 12, pp. 823–837.

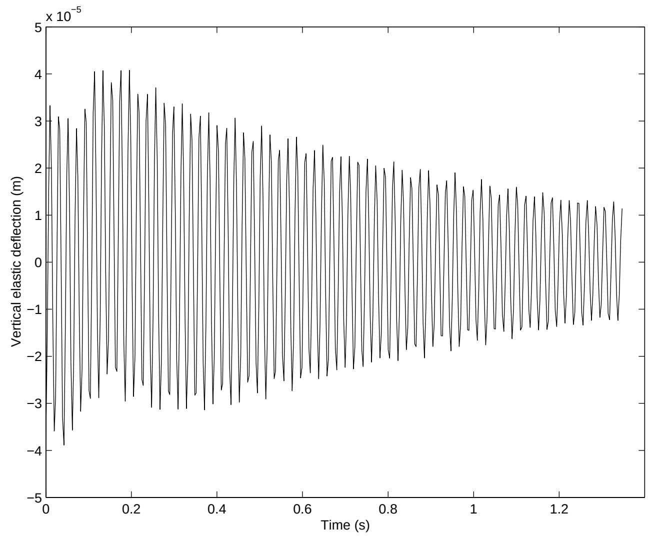

Figure 9: Midspan of link 2, vertical displacement, filtered step response

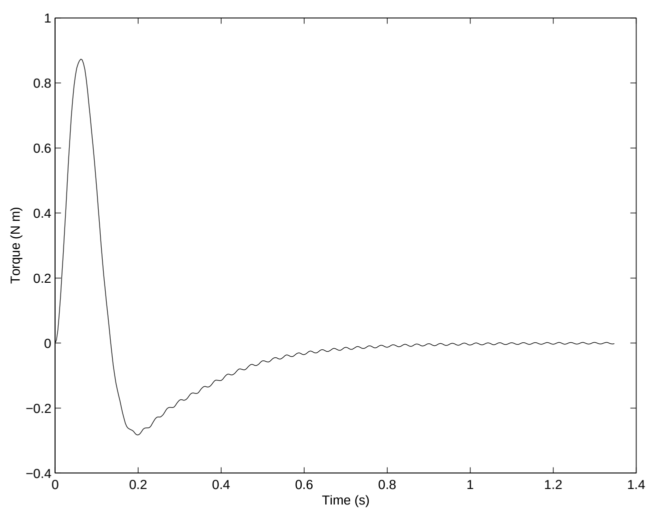

Figure 10: Applied torque, filtered step response